Evaluation on the TBM Performance at a Hydropower Project in Ecuador

K.K. Panthi and J. Encalada

K.K. Panthi J. Encalada

Abstract: The aim of this manuscript is to discuss the Tunnel Boring Machine (TBM) performance along the recently constructed headrace tunnel of Minas-San Francisco Hydropower Project in Ecuador. Firstly, the manuscript briefly describes the importance of TBM tunneling and about the Minas-San HPP. Further, discussions are made on the engineering geological conditions along the headrace tunnel. Detailed evaluations are made on the performance of TBM tunneling considering influence of rock mass quality on the TBM penetration rate. The manuscript emphasizes that the knowledge of the rock mass quality parameters and cutter technology available at present are among the key factors that influence the estimation of the net penetration rate of the TBM. It has been demonstrated that the hard to very hard rock masses of high abrasivity that were encountered along the headrace tunnel alignment caused very low penetration giving slow progress, which was not predicted during planning phase design. The authors investigated a fairly good link between TBM penetration and the mechanical strength of the rock mass.

Keywords: Tunnel Boring Machine, tunneling, Ecuador

Introduction

For the construction of long tunnels, TBM excavation shortens the excavation time and reduces the construction costs considerably compared to the drill and blast method given that, no geological surprises that cause stoppage of the excavation are met. Since TBM excavation enhances the smoothness of the tunnel contour and is circular in shape, it considerably reduces hydraulic headloss in water conveying hydropower tunnels. Therefore, TBM excavation is a preferred tunneling method for hydropower projects with long water conveying tunnels, such as headrace and tailrace tunnels.

In general, it is believed that the advance rate of a TBM excavation is less dependent on the rock mass strength, and rather on the intensity of jointing and jointing persistence. Hence, Bruland (2000) emphasized that the joints with negligible or no shear strength are indeed involved in TBM boring. The degree of fracturing is represented by a fracture class, which is classified between 0 and VI, where class category 0-II are frequently observed in rock mass such as quartzite and gabbro. Macfarlane et al. (2008) emphasized that very low penetration rate in igneous rocks are mainly characterized by the fracture class zero. On the other hand, cutter penetration in metamorphic rocks analyzed by Yagiz (2008) produced results that are insensitive of the fracture class described by Bruland (2000). Regarding fracture orientation, relatively small angle between tunnel axis and fracture planes is the most favorable condition for boring.

The advance rate is also affected by abrasiveness of minerals such as quartz, feldspar and epidote, which can also influence the usable life of the cutters. According to Dammyr (2017), in recent years, 19-inch cutters are used to achieve high thrusts and to extend the time of the cutter change to tackle problem of high abrasion. In regard to the character of the rock mass, it has been found that penetration increases as DRI and thrust per cutter increase (Movinkel and Johansen, 1986). This relationship has become fundamental for the development of prognosis models such as developed at NTNU (Bruland, 2000). Other models such as Q-TBM (Barton, 2002) incorporate mechanical strength and rock mass quality. It is acknowledged by Barton (2009) that Q-values exceeding 100 can represent difficult ground conditions for a TBM, a situation that makes the penetration mode dependent on the available power.

Mechanical breaking of rock using disc cutters involves penetration and crack propagation. In the first place, high thrust generates grooves of 1-15 mm as the cutter passes. Later on, tensional cracks are developed when the grooves are deep enough, causing spalling and consequently chipping of the rock. The development of tensile fractures will depend on the toughness of the rock. According to Whittaker et al. (1992), for disc cutters, cracks will develop in a mixture of tensional (mode I) and edge-sliding (mode II). It is important to understand that fracture toughness, which is known as the critical stress intensity factor, is the resistance to microscopic separation and cracking (Shen et al., 2014). Whittaker (1992) also shows that, values of toughness are correlated to the uniaxial compressive strength. Similarly, Atkinson (2015) associated toughness to the fracturing process of materials where the effect of loads is either static or dynamic (percussive). According to Bruland (2000), the net penetration rate of a TBM cutter head is a function of the machine and rock parameters.

The effect of the machine parameters under diverse geological conditions is represented by the penetration index (PI) and it has been widely analyzed by using records of mechanical excavation by Hassanpour et al. (2011). Bilgin et al. (2006) presented good correlations of PI with the mechanical strength of rock. In their study, penetration increases as the UCS and DRI increase. The same behavior is reported by Zare Naghadehi and Ramezanzadeh (2017), who highlighted the need for high thrusts to achieve a reasonable level of penetration in massive and strong rocks. In addition to penetration index (PI), the specific energy (SE) measured in kW/m^3 will give an idea on the capability of the equipment. The advance rate is linked to specific energy and parameters such as the rotational speed (rpm), the geometry of the cutters and the cutting power determines the level of specific energy. Cutter spacing plays a role in optimizing the level of energy. A small spacing between the cutters will compromise the cutting tools due to excessive abrasion, and a wide distance between the cutters will cause a lack of interaction and poor fragmentation. Thus, reaching an optimum energy depends on the configuration of cutting tools (Harrison and Hudson, 2000). Curves of SE for a variety of rock specimens reported by Bilgin et al. (2006) show a relation between the optimum SE and uniaxial compressive strength (UCS) of the rocks, which indicates a need for high level of energy for strong rocks. Therefore, the main aim of this manuscript is to evaluate impact of geological and machine parameters of TBM excavation and performance. The manuscript attempts to establish relations between geological, rock mechanical and machine parameters to facilitate planning of new TBM tunnels.

The Minas San-Francisco Hydropower Project

The concept of firm energy is relevant in Latin-American countries, especially in Ecuador. This geographic location is characterized by high annual runoff and a difference in topographic elevation. As a result, large hydropower systems have been and are being developed across the Andean region. The Minas San-Francisco Hydropower Project (MSF HPP) was recently implemented at the southeast region of Ecuador. The project has an installed capacity of 275 MW and produces 1290 GWh energy annually (MEER, 2018). As shown in Figure 1, the main features of the project consist of an RCC dam of 77 m height (measured from the foundation), a 12 km low pressure headrace tunnel, a penstock shaft, and an underground power station equipped with three pelton turbine units. The implementation of the MSF HPP started in 2012 and was extended until February 2018 (Torres et al., 2011).

In the context of large hydro power projects, three critical components are always in the focus of analysis; i.e. headworks, waterway system and the underground power station. In the case of waterway system, tunneling techniques are influenced by the rock mass conditions and the extent of the excavation. Thus, cost-effective solutions in long tunnels include the use of tunnel boring machines (TBMs). For the MSF HPP, a 9 km headrace tunnel was excavated using a double shield TBM. An interesting aspect of the excavation was the low advance rate experienced in this project, despite in-depth knowledge on the character of the rock mass in the design stage.

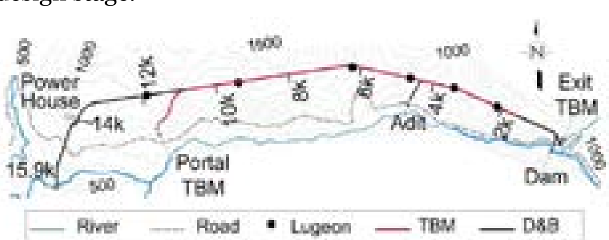

Figure 1. Main features of the MSF HPP (reproduced from Torres, 2011; Bedoya and Suescun, 2014; Jimenez, 2014)

In the area of the reservoir, rocks of volcanic origin with some intrusions of quartz-monzonite are common with their average strength of about 50MPa, and GSI values ranging from 60 to 80 (Riemmer et al, 2013). The segment of the headrace tunnel on the other hand is distinguished by zones of volcanic and plutonic rocks. The TBM excavation with a cross section diameter of 5.76 m took place in both rock types between chainages 10.8 km and 1.6 km (Torres et al, 2011). The location of adits and portals used for the excavation are shown in Figure 1. Rocks such as gabbro and andesite prevailed along the segments excavated by the TBM. Only last segment of excavation from chainage 2 km is composed of tuff and breccia of volcanic sediments. A low performance was experienced, especially when excavating intrusive rocks. In the case of the MSF HPP, 19-inch cutters allowed the application of loads up to 300 kN per cutter, reaching the nominal capacity of steel (Della Valle, 2015).

Excavation with TBM

Daily records of parameters such as UCS, water inflow, average cutter thrust, and rotational speed (rpm) are used in this analysis. Useful results from the feasibility stage are taken as to complement the present work. It is already known that the uniaxial compressive strength of the rock varied widely along the tunnel alignment. In the same way, previous analysis shows that most sections of the TBM tunnel satisfy the Norwegian criteria for minimum rock cover (Riemmer et al, 2013). In regards to potential inflow in the tunnel, it was observed that the ground water table is relatively deep with no as such water ingress observed in the tunnel, excluding boreholes located at the reservoir area (Suescún and Jiménez, 2017).

Types of rocks and their character

The rocks excavated were andesite, hornfels, gabbro, diorite, volcanic breccia and alternated layers of tuff and shale (Figure 2). Andesitic dykes – are oriented N-E and dipping 70° NW and these dykes appear sporadically. The Cerchar Abrasivity Index (CAI) for rock specimens tested during excavation show that andesite was abrasive to extremely abrasive, gabbro very abrasive, and the sedimentary rocks were abrasive (Suescún and Jiménez, 2017). Hornfels was observed sporadically and no CAI was available for this rock.

It was seen that the abrasiveness determined during construction was not different from values reported in feasibility studies; neither do DRI values show discrepancy.

Figure 2. Main geological features along the tunnel alignment (reproduced from Torres et al.,, 2011; Bedoya and Suescun, 2014; Jimenez, 2014)

Furthermore, the rocks described above are characterized by having porosities below 1% having dominating minerals of quartz and epidote.

Weakness zones and discontinuities

A single shear zone of 20 cm thickness was met at chainage 6.0 km belonging to the hydro-thermally altered zone, a shear zone of low cover (Suescún and Jiménez, 2017). This finding greatly differs from the idea of thrust faults with altered bands of 3 m thickness described in the feasibility study and detailed design. Otherwise, joint surfaces in the rock mass along the tunnel alignment was found to be rough, undulating and relatively tight. More than half of the joints were found to be filled with quartz particles, while remaining joints were found to be filled with some staining or without infilling, but very tight. In addition, the weathering was very limited with a weathering grade of fresh rocks (W1) according to ISRM (1978). This condition is important because weathering can affect the mechanical strength of the rock according to Panthi (2006). Suescún and Jiménez (2017) also found that borehole logs and reports during excavation classify most of the rock as fresh rocks. The jointing intensity and their orientation is presented in Figure 3. The records of registered jointing condition along the TBM tunnel provides possibility to characterize tunnel segments of interest. As one can see in Figure 3 (right), there are mainly three system of joint sets; i.e. Jn1, Jn2 and Jn3. The joint systems are strongly dipping along the whole tunnel, a situation that is considered unfavorable for the advance rate.

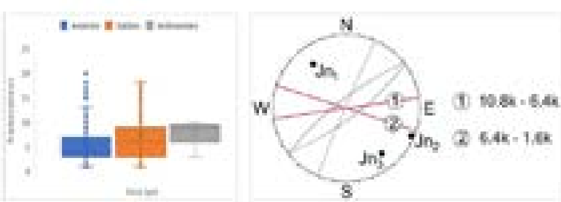

Figure 3. Fracture frequency and orientation along the TBM tunnel (plotted based on Torres et al., 2011; Suescún and Jiménez, 2017).

It is also important to highlight here that the degree of fracturing has been analyzed in terms of RQD rather than only fractures per meter. The problem is that classification based on the mean spacing value (fracture frequency) is limited and the concept of RQD in solving this problem has been used. Effectively, this study made use of a probability density function (pdf) that replicates the natural clustering of fractures according to Harrison and Hudson (2000) that considers small spacing values occurring more frequent than the one with large spacing (Figure 3, left).

Compressive strength

The strength of the intrusive hard to very hard rock varies greatly depending upon weathering condition and grain size distribution. The UCS records of 216 tested specimens from along the tunnel is presented in Figure 4. Hornfels exhibit an extremely high resistance to compression. As discussed previously, Hornfels and Diorite appeared sporadically at chainages 9.9 km and 10.1 km in segments of 20 m and 85 m, respectively.

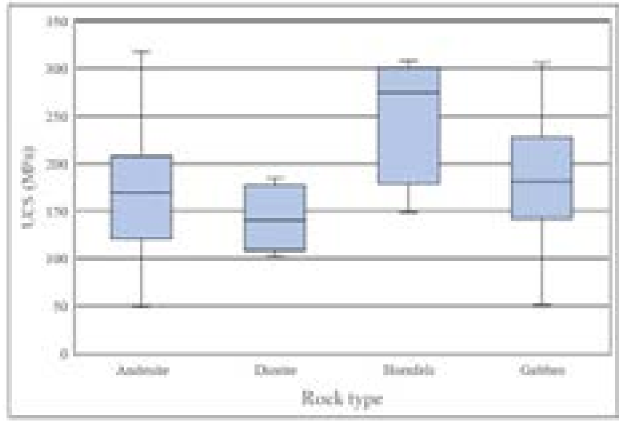

Figure 4. Compressive strength for the rocks along TBM tunnel (based on Suescún and Jiménez 2017).

For volcanic and sedimentary rock formations, the compressive strength can be inferred from tests reported in the reservoir area where typical mean value was found to be around 50 MPa (Suescún and Jiménez, 2017). This observation is correct as high penetration rates were achieved in these rock formations.

Rock mass quality

The geological mapping along the tunnel resulted the rock quality to be much superior to the values predicted at feasibility and detailed design stages. Figure 5 gives distribution of predicted and actual RMR class according to Bieniawski (1989). Since double shield TBM with continuous concrete segment lining was used, rock mass class was not used for tunnel support design.

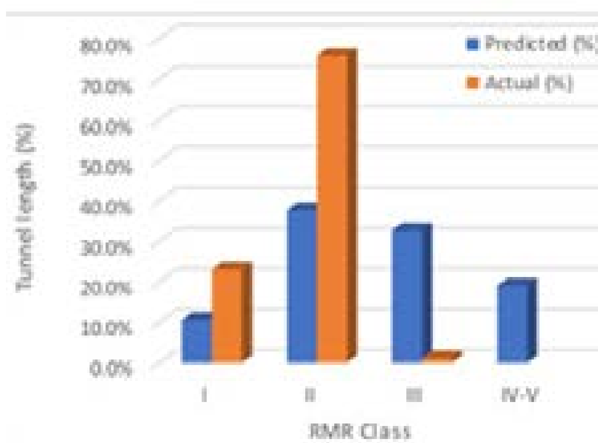

Figure 5. Actual and predicted rock mass class based on mapped RMR values.

As one can see in Figure 5, much better quality of rock mass was registered along the tunnel alignment than that was predicted. The high rock mass quality class experienced has direct influence on the production rate of the TBM.

Cutter thrust

For the analysis of the advance rate, 29 single cutters and 4 twin-cutters contained in the cutter head were studied independently with a consideration on the analysis of average thrust per cutter. The simplified version of the prognosis model suggested by Barton (2009) and Bruland (2000) was utilized for this purpose. This was also justified with field observations of the performance of disc cutters. The cutter rings sent to the garbage store showed signs of failure of the steel, indicating working conditions close to the nominal capacity of 300 kN. Della Valle (2015) noted that the whole thrust was concentrated mainly on the frontal cutters. Therefore, load on peripheral cutters was disregarded for the evaluation of average thrust per cutter.

Operational capability

In TBM excavation, about 1 km tunnel including part of the adit TBM can in general be considered to gain experience. It can be seen in Figure 6, despite a rotational speed of 6-7 rpm and cutter thrust of 300 kN, the penetration significantly dropped by April 2015 at chainage 10 km.

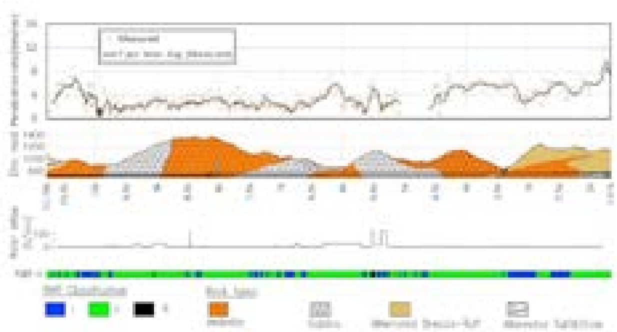

Figure 6. Penetration and rock mass conditions (based on Torres et al. 2011; Suescún and Jiménez 2017).

Since the beginning of the excavation in December 2014 until April 2015, the production dropped gradually from 544 to 41 m³/cutter. In the zone of low production, the rocks consisting of dykes of hornfels and gabbro were encountered. The change of rings was frequent, which mostly indicated failure on the steel. The average consumption of the cutter ring was approximately 54 per month according to Della Valle (2015). The drop in the production was caused by failure of a twin cutter housing, representing large fissures on the steel, which was finally solved in August 2015 after reaching the chainage 6 km.

Behavior of penetration under varied geological conditions

The penetration rate recorded is shown Figure 6. Two extremes can be observed in Figure 6; i.e. massive and relatively fresh gabbro at chainage 9.6 km and slightly weathered volcanic sedimentary rock formations at chainage 1.7 km. It is clear that the excavation process is subject to inaccuracies in operation and sampling data. It was also found that the strength of rock had high variability locally, causing fluctuation on the global tendency.

The effect of mechanical failure in between the chainage interval of 10.1 km - 9.02 km can be easily observed and it is reasonable to exclude this data for further analyses. Based on reliable records, three aspects of TBM performance can be pointed out. First, the penetration is to some extent related to the depth of overburden due to the degree of fracturing, which is in general higher at shallow depths. Secondly, the rock mass quality is related to the penetration rate as observed at chainages 3 km and 5.5 km having a low performance for rock mass class category I and a noticeable increase in penetration rate for rock mass class category III. Thirdly, the change in advance rate from igneous to sedimentary rocks is also noticeable, which can be attributed to the lower mechanical strength of the sedimentary rock formations. The effect of the mechanical strength on the penetration can also be seen

in chips product of excavation (Figure 7), revealing the high level of toughness of the intact rock.

Figure 7. Chip product of excavation at chainage 10.14 km (Suescún and Jiménez, 2017).

According to Suescún and Jiménez (2017), most chips were of 1-3 cm thickness, 5-10 cm wide, and 10-20 cm in length. The specimen shown in the figure is no more than 15 cm in length and represents a zone of favorable borability. However, throughout the excavation, most chips presented small, planar and angular shapes, indicating a low cutting power compared to the exceptional characteristics of the rock encountered.

Inflow and leakage

It was observed in Figure 6 that a relatively high inflow of 25 - 125 ltr / min was met in two occasions. The first one, near to zones of rock type III at chainage 5.5 km and the second one at 8.5 km. Overall inflow and leakage conditions of the tunnel are reflected on the mean permeability observed after several lugeon tests. Along the tunnel, permeability varied between 1.6 × 10-7 and 4.2 × 10-8. Inflow measurement during construction was not required because of the wide knowledge of the permeability beforehand. Measurement of water leakage also reveals a very low leakage with a mean value of 1.2 ltr/min/m and a maximum leakage of 3.6 ltr/min/m.

Analysis and Discussion

Data from the penetration rate (mm/rev) was analyzed in terms of the parameters discussed above. An attempt was made to find out a correlation between the TBM penetration rate and degree of fracturing represented by RQD (Figure 8, left). As one can see in the analysis plot, there exists very poor correlation. This is quite logical since the RQD is a value represented by length of cores longer than 10 cm in a one-meter drilled core, which may sometimes give false information on the jointing condition in the rock mass. For example, a rock mass having joint system spaced slightly over 10 cm can give an RQD value exceeding 80. On the other hand, the same rock mass having joint spacing slightly lower than 10 cm will end with RQD value below 20. Hence, only RQD is not enough of a parameter to estimate TBM penetration rate. Similarly, a correlation between penetration rate and UCS was also assessed, which resulted an improvement on the correlation (Figure 8, right). However, the improvement is not that significant either.

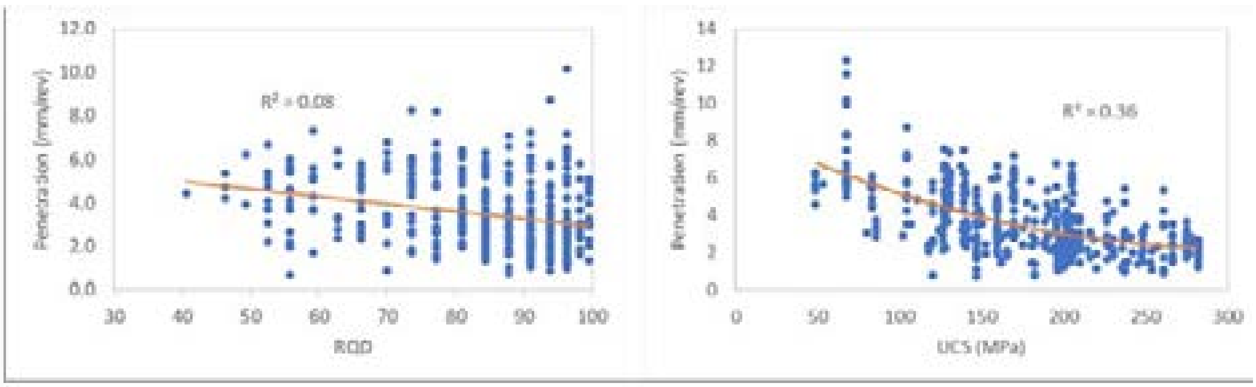

Figure 8. Penetration rate in relation with RQD (left) and UCS (right).

Further attempt was made to find a correlation between the ratio of thrust and penetration rate, which represents Penetration Index (PI) with the multiplication of UCS and RQD (Figure 9, left). Both lab tested UCS results of 216 specimens, estimated UCS at the tunnel and mapped RQD values were used for this purpose. As one can see, a fairly good correlation was found. Similarly, it was found that there exists a good correlation between Specific Energy (SE) with the multiplication of UCS and RQD values (Figure 9, right).

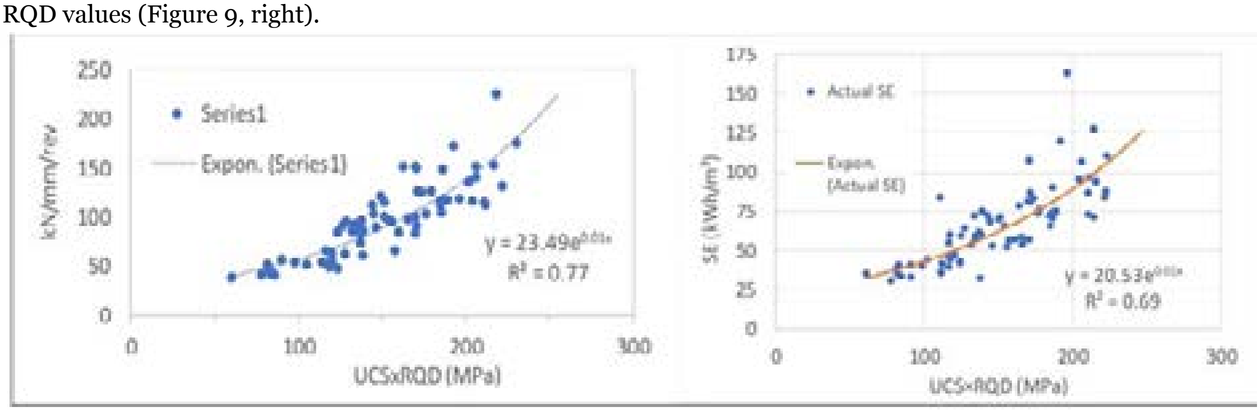

Figure 9. Penetration Index (PI) (left) and Specific Energy (right) in relation with RQD multiplied by UCS.

The findings of Figure 9 have significant importance in estimating Penetration Index (PI) and Specific Energy (SE) for the tunnels passing through similar geological conditions. The relationship achieved here can be further enhanced and improved using data and information of the TBM performance of other TBM tunnel projects built in other geological environments. In addition, the effect of abrasiveness can also be seen in the form of gross advance rate (Figure 10).

Figure 10. Weekly utilization and gross advance rate (based on data from Suescún and Jiménez, 2017).

The damage produced to the twin cutter host affected the gross advance from Week 8 to Week 30. During this time lapse, the advance was low in spite of high utilization of the machine. As indicated in Figure 10, a change of disc cutter took place during March 2016 (Weeks 57-58) at chainage 6+800, which clearly indicates noticeable drop in the advance rate. It can also be seen in the figure that the production was considerably improved for the same utilization time when the excavation approached sedimentary rock formations with enhanced borability characteristics.

Despite the favorable mechanical properties of the rock mass along the TBM tunnel, permanent concrete lining was used at this project based on the recommendation made in the design and contract documents where double shielded TBM was recommended. Most segments of the tunnel that were excavated using TBM, showed a great advantage in terms of stand-up time with high quality rock mass and low permeability. Experience on the use of unlined high-pressure shafts and tunnels in Norway (Benson, 1989; Buen and Palmstrom, 1982; Broch, 1982; Panthi, 2014; Basnet and Panthi, 2018) suggests that permeability and rock mass quality similar to this case should have been suitable for the implementation of unlined pressure tunnel concept developed in Norway. A second project downstream of the MSF HPP is to be developed and part of it will follow the rock formation dominated by granitic gneiss and quartzite. This condition should be considered as a possible choice of the implementation of unlined medium to low pressure headrace tunnel.

Conclusions

The engineering geological parameters in relation with both TBM Penetration Index (PI), Specific Energy (SE) and the advance rate of TBM at MSF Hydropower Project have been analyzed. The analysis concludes that there exists fairly good correlation between Penetration Index (PI) and Specific Energy (SE) with the multiplication of RQD and UCS. The proposed correlation can be enhanced by using TBM performance data and information from other TBM projects having different geological environment. However, it is emphasized here that care should be taken while using the proposed correlations since they represent from only one single TBM project.

– –

Dr. Krishna Kanta Panthi*, Associate Professor of Geological Engineering and Expert in Engineering Geology, Tunneling and Hydropower, has over twenty five years of experience in identification, feasibility assessment, design, construction management, inspection and research in rock engineering, tunneling, hydropower, other civil engineering and mining projects. He poses extensive theoretical, practical and commercial understanding of tunneling and renewable hydropower projects including due diligence, risk management and contractual management.*

Corresponding address: krishna.panthi@ntnu.no

Mr. Jhonny Encalada *has recently completed his MSc study in Hydropower Development from the Norwegian University of Science and Technology (NTNU), Trondheim, Norway in 2018. Mr. Encalada has over 5 years of experience in construction and design of tunneling and hydropower projects. Currently, he works as consulting engineer in Ecuador.*

References

Atkinson B. K. 2015. Fracture Mechanics of Rrock. *Elsevier.*

Barton N. 2002. Some New Q-value Correlations to Assist in Site Characterization and Tunnel Design. *International Journal of Rock Mechanics and Mining Sciences* (39): 185-216.

Barton N. 2009. TBM Prognoses in Hard Rock with Faults using Q TBM Methods. *IoM3 Institute of Materials, Minerals & Mining.* Hong Kong.

Basnet C. B. and Panthi K. K. 2018. Analysis of Unlined Pressure Shafts and Tunnels of Selected Norwegian Hydropower Projects. *Journal of Rock Mechanics and Geotechnical Engineering* (10): 486-512.

Benson R. P. 1989. Design of unlined and lined pressure tunnels. *Tunneling and Underground Space Technology* (4): 155-170.

Bedoye R. and Suescun C. 2014. Informe Tecnico Horizonte de Toba Limolitika Cinerita – Caverna Casa de Maquinas. *Minas-San Francisco Hydropower Project.* Ecuador.

Bieniawski Z. T. 1989. Engineering Rock Mass Classifications: A Complete Manual for Engineers and Geologists in Mining, Civil, and Petroleum Engineering. *Wiley.*

Bilgin N., Demircin M. A., Copur H., Balci C., Tuncdemir H. and Akcin N. 2006. Dominant rock properties affecting the performance of conical picks and the comparison of some experimental and theoretical results. *International Journal of Rock Mechanics and Mining Sciences* (43): 139-156.

Broch E. 1982. The Development of Unlined Pressure Shafts and Tunnels in Norway. *ISRM International Symposium*. Aachen, Germany.

Bruland A. 2000. Hard Rock Tunnel Boring. *Advance Rate and Cutter Wear* (3).

Buen B. and Palmstrom A. 1982. Design and Supervision of Unlined Hydro Power Shafts and Tunnels with Head up to 590 meters. *ISRM International Symposium*. Aachen, Germany.

Della Valle N. 2015. Informe de la visita realizada por el Dr. *Nicola Della Valle*. CELECEP.

Dammyr, Ø. 2017. Evaluation of the potential for TBM use in future Norwegian Tunneling Projects. *PhD thesis*. Norwegian University of Science and Technology (NTNU).

Harrison J. P. and Hudson J. A. 2000. Engineering Rock Mechanics: An Introduction to the Principles. *Elsevier Science*. Burlington.

Hassanpour J., Rostami J. and Zhao J. 2011. A New Hard Rock TBM Performance Prediction Model for Project Planning. *Tunneling and Underground Space Technology* (26): 595-603.

ISRM. 1978. Technical Introduction. *International Journal of Rovck Mechanics and Mining Sciences & Geomechanics Abstracts* (24): 124-134.

Jimenez C. 2014. Registro Geologiko Geotecnico CDM 5. *CELECEP*.

Macfarlane D. F., Watts C. R. and Nilsen B. 2008. Field Application of NTH Fracture Classification at the Second Panapouri Tailrace Tunnel. *New Zealand*.

MEER. 2018. *Proyecto Hidroelectrico Minas – San Francisco*. Ministreio de Electricidad y Energia Renovable. Ecuador.

Movinkel T. and Johansen O. 1986. Geological Parameters for Hard Rock Tunnel Boring. *Tunnels and Tunneling*.

Panthi K. K. 2006. Analysis of Engineering Geological Uncertainties Related to Tunneling in Himalayan Rock Mass Conditions. *PhD Thesis*. Norwegian University of Science and Technology. Trondheim.

Panthi K. K. 2014. Norwegian Design Principle for High Pressure Tunnels and Shafts: It's Applicability in the Himalaya. *Hydro Nepal* (14): 36-40.

Riemmer W., Forbes B., and Villegas F. 2013. Proyecto Hidroelectrico Minas-San Francisco: Informe1-Panel de Consultores. Enerjubones.

Shen B., Stephansson O. and Rinne M. 2014. Modelling Rock Fracturing Processes: A Fracture Mechanics Approach using FRACOD.

Suescún C. and Jiménez, C. 2017. Geologia Tunnel de Conduccion. *463-IT-017-A*. CELECEP.

Torres L. and Vega G. 2011. Proyecto Minas – San Francisco-Informe de Geologia y Geotecnia – Evento 7, Estudio Geológico Definitivo. *Enerjubones Generadora Hidroelectrica.* Ecuador.

Whittaker B. N., Singh R. N. and Sun G. 1992. Rock Fracture Mechanics: Principles, Design and Applications. *Elsevier.* Amsterdam.

Yagiz S. 2008. Utilizing Rock Mass Properties for Predicting TBM Performance in Hard Rock Condition.

Zare Naghadehi M. and Ramezanzadeh A. 2017. Models for Estimation of TBM Performance in Granitic and Mica Gneiss Hard Rocks in a Hydropower Tunnel. *Bulletin of Engineering Geology and the Environment* (76): 1627-1641.